The Effects of Dwell_time of Monopolar Waveform on Droplet Formation through the Analysis of Fluid Propagation Direction

Cheng-Han Wu* and Weng-Sing Hwang**

*Department of Materials Science and Engineeing, National Cheng Kung University, Tainan City 701, Taiwan, R.O.C., semajwu@gmail.com
** Department of Materials Science and Engineeing, National Cheng Kung University, Tainan City 701, Taiwan, R.O.C., wshwang@mail.ncku.edu.tw

ABSTRACT

The fluid dynamics in a capillary tube caused by the movement of the piezoelectric material is essential for inkjet printing due to the need for adjusting the voltage pulse waveform, but it has seldom been observed and measured. This study investigates the pressure wave propagation of molten solder induced by a voltage pulse using a numerical simulation method. Micro droplets of molten lead-free solder, Sn3.0Ag0.5Cu, were ejected at 230 ℃ using a squeeze-mode piezoelectric inkjet printing process. Simulation results, which were verified by experiment results, show the insufficiency for explaining the droplet behavior with conventional pressure superposition, considering the droplet behavior with the use of the fluid propagation direction is a more comprehensive analysis method to evaluate the droplet formation type.

Keywords: propagation direction, lead-free solder, numerical simulation, droplet formation, dwell_time

1 INTRODUCTION

Lead-free solder by inkjet printing technique has been applied on the electric package industry for the past few decades. Compare to the conventional fabrication method, inkjet printing possesses advantages such as few fabrication procedures, reduction of time consumption, and cost efficiency. However, adjusting the parameter when operating a piezoelectric device at high temperature is imperative, therefore, understanding the effect of the parameter on the droplet formation is essential.

Many researches found that the optimum dwell_time of a monopolar waveform can be obtained through determining droplet velocity, droplet size or meniscus motion [1-3]. Kwon [4] used self-sensing technique to measure the pressure in the capillary tube and analyzed it with Bogy's wave propagation theory. Laser Doppler vibrometer (LDV) has also been applied in measuring the bending deflection of the piezoelectric actuator by Kim [5].

The present study investigates the effects of the dwell_time of a monopolar waveform on molten solder droplet formation by a squeeze mode inkjet printing through the analysis of fluid propagation direction using experiments and simulation.

2 NUMERICAL MODEL

2.1 Physical Model

A commercial computational fluid dynamic software, Flow-3D, was applied in the numerical model. A cylindrical symmetric system was used to make meshes. In Fig.1, meshes were made as the shape of a tube with a nozzle. At the boundary of the tube wall, there was a moving object along the r direction which was considered as the piezoelectric actuator.

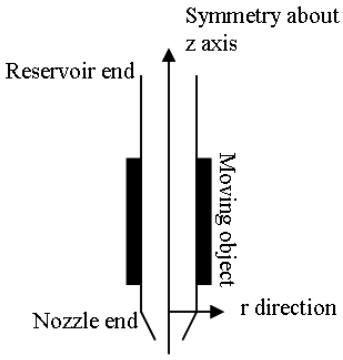

Figure 1: A schematic illustration of the numerical model.

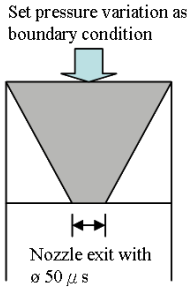

Figure 2: A schematic illustration of a nozzle with denser mesh. The pressure variation was set as a boundary condition on the top of the nozzle.

A pressure may be generated by the moving object, and the pressure variation at the nozzle can be downloaded and input to another model shown as Fig. 2 as a boundary condition. The model in Fig. 2 possesses denser mesh in order to sketch the contour of the droplet more detail.

2.2 Governing Equation and Boundary Condition

The Navier-Stokes equation of momentum and continuity were used to govern the Newtonian fluid. The mass continuity equation, the laminar equation of motion, and the equation for fluid fraction were applied to control the fluid flow. The volume-of-fluid method was used to track the free surface. The gravity was neglected due to its small influence. The following boundary conditions were specified:

- Symmetry about z axis;
- No-slip at the solid boundary;
- Free surface;
- Specified pressure at the reservoir end.

3 EXPERIMENTAL METHOD

3.1 Apparatus and Material

The illustration of the apparatus is shown in Fig. 3. The piezoelectric device was controlled with a printing system, which gave voltage pulse and time interval of a waveform to the device, and also controlled the inkjet frequency. In order to eject the molten solder, a heating system was required to melt the lead-free solder. A pneumatic system was used to supply N_2 as backup pressure and the shroud flow near the orifice. There is still monitoring system used to observe the droplet evolution. An LED lamp with delay time controlled by software and a CCD camera are included in the monitoring system.

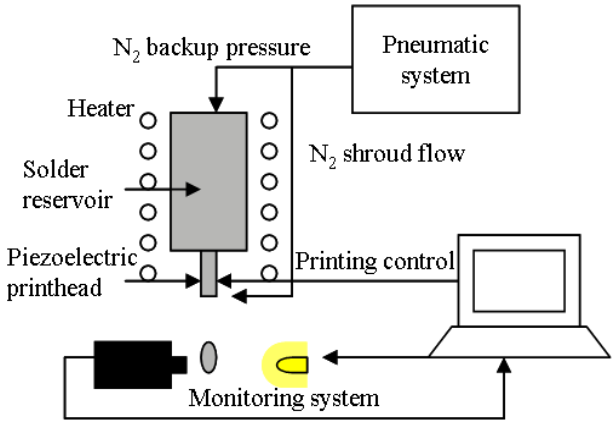

Figure 3: The illustration of the apparatus.

The lead-free solder, Sn-3.0wt%Ag-0.5wt%Cu, was used as the ink material. Its solidus temperature is 211℃ and liquidus temperature is 217℃.

3.2 Inkjet Printing Conditions

A monopolar pulse waveform was applied on the piezoelectric device. There are three time intervals, which denoted as t_{rise}, t_{dwell} and t_{fall}. At t_{rise}, there was a positive voltage change of 5V. After a delayed time of t_{dwell}, a negative voltage change of 5V was applied. The values of t_{rise} and t_{fall} were set as 4μs. The droplet formations were observed under various t_{dwell}. The solder was heated up to 230℃. The backup pressure was set as 1.0kPa and the shroud flow was about 1 L▪min^{-1}.

4 RESULT AND DISCUSSION

4.1 Experimental Observation

X (μs)	Phenomena
0-6	Chaos droplets were produced and stuck around the nozzle easily, which accumulated as a big drop.
7-14	Droplet cannot be produced.
15-23	Single droplet was produced.
24-	Low speed single droplet was produced and stuck around the nozzle easily with the interference of surroundings.

Table 1: The four droplet formation types with various t_{dwell} value; the time interval of t_{rise}_t_{dwell}_t_{fall} is 4_X_4μs.

Droplets were produced by a piezoelectric mode inkjet printing device with various t_{dwell} of the monopolar pulse waveform. Each droplet was recorded by CCD camera with each t_{dwell}. Data compilation is shown in Table 1. There are four droplet formation types with various values of t_{dwell}. For the first type, chaos droplets were ejected out of the nozzle with the values of t_{dwell} between 0 to 6μs. The small chaos droplet was easily interfered by surrounding air flow, and stuck around the nozzle. Therefore, the chaos droplets accumulated as a big drop at nozzle. The big drop fell eventually when the weight of the drop is larger than its surface tension at the orifice. For the second type, there is no droplet formation with t_{dwell} between 7 to 14μs. The meniscus of liquid front was pushed out of the orifice first, and then, withdrawn back into the orifice. No droplet was produced at this range of t_{dwell} values. For the third droplet formation type, a single droplet can be produced with t_{dwell} between 15 to 23μs. The droplet speed increased as t_{dwell} from 15 to 18μs. It reached a maximum speed with t_{dwell} = 18μs, and then, decreased with the increase of t_{dwell}. Finally, with the increase of t_{dwell} up to 24μs, the low speed droplet was produced. The phenomenon of the low speed droplet is similar with that of the first droplet formation type. The

droplet moved slowly near the nozzle exit and easily stuck around the nozzle due to the interference of surroundings. The value of t_{dwell} obviously influences the droplet formation morphology. A t_{dwell} value of each type was chosen as the simulation parameter.

4.2 Simulation Results

The simulation results of four droplet formation types are shown in Fig. 4. For the droplet formation evolution of t_{dwell} = 6μs, the liquid front was withdrawn first, and then, pushed out of the nozzle. After that, an obvious withdrawn liquid front appeared and the liquid thread was broken as a very small droplet, which was same as the situation of the first droplet formation type mentioned above. However, it is an ideal condition within the simulation, so there is no external influencing factor, which could make the droplet stick on the nozzle. For the droplet formation evolution of t_{dwell} = 12μs, after the liquid front was withdrawn and pushed out of the nozzle, all liquid was pulled back into the nozzle, and there was no droplet formation. For that of t_{dwell} = 18μs, the pushed liquid thread was pulled back appropriately, and a single droplet was formed. For the droplet formation evolution of t_{dwell} = 24μs, the pushed force was obviously smaller than that of t_{dwell} = 18μs. The pinch-off process was slower, and the flying speed was also slower. From the simulated droplet formation evolution, it shows that the simulation results were validated by the experiment ones. The data from simulation can be used to analyze the mechanism of droplet behavior.

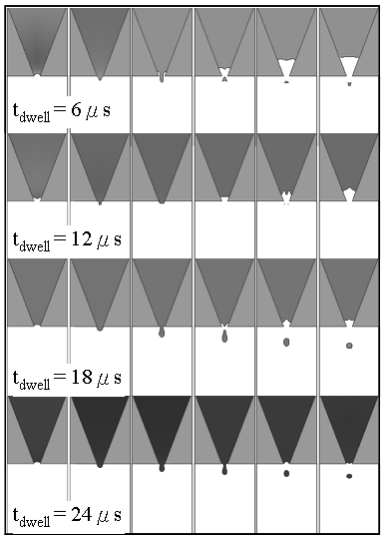

Figure 4: Simulated droplet formation evolutions of four droplet formation types with t_{dwell} = 6, 12, 18 and 24μs.

The calculated pressure at the nozzle induced at t_{rise} only is shown in Fig. 5. Based on the lab previous work, it revealed that two pressure waves induced at different time intervals can roughly superpose to each other and make the hypothetic structure of the pressure variation. Therefore, the calculated pressure induced at t_{rise} in Fig. 5 was used to describe how the t_{dwell} would work on the change of the whole pressure variation. Before that, the structure of the pressure wave induced at t_{rise} should be interpreted.

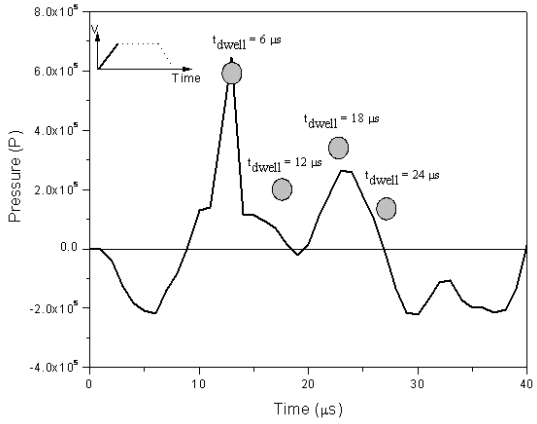

Figure 5: The calculated pressure variation at nozzle induced at t_{rise}.

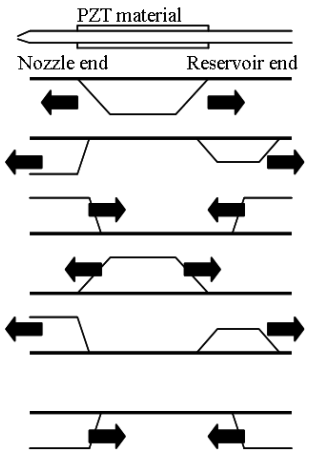

Figure 6: An illustration of a negative pressure wave propagation along the capillary tube.

Fig. 5 shows the pressure variation at the nozzle with time. When the piezoelectric actuator received a positive voltage change at t_{rise}, the piezoelectric material contracted and gave the chamber a negative pressure like that in Fig. 6. Fig. 6 is an illustration of how the fluid propagation works. A negative pressure was induced within the chamber in the beginning, and then, propagated toward both ends, namely the nozzle end and the reservoir end. In the lab previous work, it showed that the negative pressure toward the nozzle end reflected as a positive pressure due to the nozzle end is not completely closed as what Bogy described. And then, the positive pressure which reflected at the reservoir end moved toward the nozzle end reflected as a negative pressure. Therefore, in Fig. 5, the pressure experienced a

negative peak, followed by two positive peaks and ended as a negative peak. According to the t_{dwell} mentioned above, the positive pressure induced at t_{fall} may appear at the grey spot position. When the positive pressure induced at t_{fall} superposed the positive peak of t_{dwell} = 6 and 18μs in Fig. 5, a large amount of liquid was supposed to be pushed out of the nozzle. However, the droplet behavior of t_{dwell} = 6μs revealed as a small chaos droplet, which implied that the pressure variation may not be the only factor to control the droplet formation mechanism.

4.3 Analysis of the Effect of Fluid Propagation Direction

In order to understand more about the droplet behavior mechanism, the effect of the fluid propagation direction on droplet formation was analyzed. The comparison of pressure and velocity variation at the nozzle is shown in Fig. 7. For the velocity variation, the positive velocity represents the direction from nozzle to the tube center, and the negative velocity means the direction out of the nozzle. In the beginning, the negative pressure was applied on the nozzle, and this coming negative pressure from the tube center leaded an increasing positive velocity, which means the fluid flowed away from nozzle and back to the center. The reflected positive pressure slowed down the positive velocity. The second positive pressure, reflected from reservoir end, leaded an increasing negative velocity, which may cause fluid to be pushed out of the nozzle. And the reflected negative pressure slowed down the velocity.

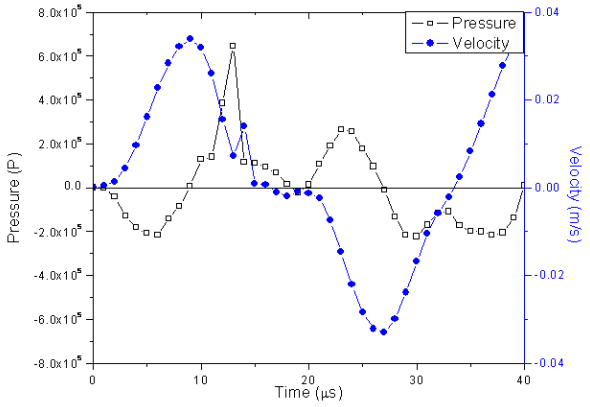

Figure 7: Comparison of the calculated pressure and velocity variation at the nozzle induced at t_{rise}.

In the Fig. 8, with t_{dwell} = 6μs, the negative velocity induced at t_{fall} didn't superpose on one that was induced at t_{rise}, and this leaded not only useless superposition, but also instability of velocity variation, which may cause unstable droplet formation. While the negative velocity induced at t_{fall} with t_{dwell} = 18μs superposed on the negative part induced at t_{rise}, and provided a large fluid propagation speed toward the nozzle, which produced a optimal droplet formation. As for t_{dwell} = 12μs, the negative velocity induced at t_{fall} also superposed on the negative part, but the following positive velocity was too large that pulled the liquid back. For the velocity variation with t_{dwell} =24 μs, the negative velocity didn't superpose very well, therefore, the droplet speed was slower.

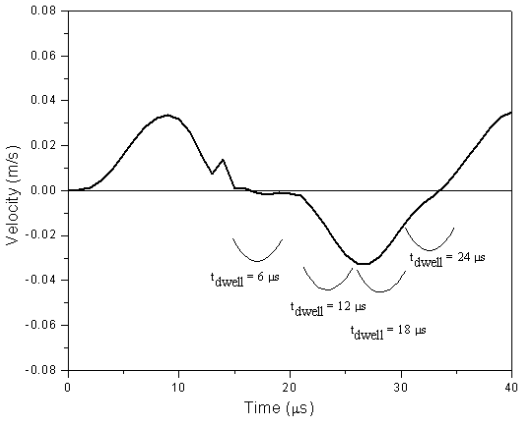

Figure 8: The calculated velocity variation at the nozzle induced at t_{rise} and the positions of the negative pressure induced at t_{fall} with various t_{dwell}.

5 CONCLUSION

Four droplet formation types, chaos droplet, non-droplet, single droplet and low speed droplet, were observed with different values of t_{dwell} in a monopolar pulse waveform in the experiment, which validated the simulation results. From the simulation results, it shows that it is insufficient to explain the droplet behavior with conventional pressure superposition, considering the droplet behavior with the use of the fluid propagation direction is a more comprehensive analysis method to evaluate the droplet formation type.

ACKNOWLEDGEMENT

This work was supported by the Research Center for Energy Technology and Strategy in Taiwan, which is gratefully acknowledged.

REFERENCES

[1] D. B. Bogy and F. E. Talke, IBM J. Res. Dev., 28, 314-321, 1984.

[2] H. Y. Gan, X. Shan, T. Eriksson, B. K. Lok and Y. C. Lam, J. Micromech. Microeng., 19, 055010, 2009.

[3] K. S. Kwon, J. Microelectromech. S., 18, 1118-1125, 2009.

[4] K. S. Kwon and W. Kim, Sensor. Actuat. A- Phys., 140, 75-83, 2007.

[5] C. S. Kim, W. Sim, J. S. Lee, Y. S. Yoo and J. Joung, IEEE International Symposium on Industrial Electronics (ISIE) in 2010, 1817-1822, 2010.